ISSN 1063-7745, Crystallography Reports, 2021, Vol. 66, No. 7, pp. 1227–1232. © Pleiades Publishing, Inc., 2021.

STRUCTURE OF ORGANIC COMPOUNDS

Synthesis, Characterization, and Crystal Structure of 3,3,6,6-Tetramethyl-9-(4-Methoxyphenyl)-10-(4-Chlorophenyl)-1,8-Dioxodecahydroacridine Dimethyl Sulfoxide

V. Sharma[a], S. Sharma[b], S. Paul[b], and V. K. Gupta[a,*]

[a] *Department of Physics, University of Jammu, Jammu Tawi, 180006 India*

[b] *Department of Chemistry, University of Jammu, Jammu Tawi, 180006 India*

* *e-mail: vivek.gupta2k9@gmail.com*

Received June 15, 2020; revised September 11, 2020; accepted September 16, 2020

Abstract—By following one-pot synthesis, an acridinediones derivative compound 3,3,6,6-tetramethyl-9-(4-methoxyphenyl)-10-(4-chlorophenyl)-1,8-dioxodecahydroacridine dimethyl sulfoxide, $C_{30}H_{32}O_3ClNS{\cdot}C_2H_6OS$ has been synthesized using a green protocol and its crystal structure is determined by X-ray structure analysis. The crystals are Triclinic with space group $P\bar{1}$, $Z = 2$. The crystal structure was solved by direct method and refined by full matrix least squares procedure to a final R value of 0.0587 for 4137 observed reflections. The pyridine ring adopts flattened boat conformation whereas both cyclohexene adopts envelope conformations. The crystal structure is stabilized by C–H···O and C–H···π hydrogen bonds involving the DMSO solvent molecule which are further understood through Hirshfeld surface analysis.

DOI: 10.1134/S1063774521070154

INTRODUCTION

Acridinediones containing 1,4-dihydropyridine nucleus along with remarkable physical and chemical properties exhibits large variety of biological activity and finds utility in pharmaceutical and dye industry. This 1,4-dihydropyridine unit shows biological activities such as neuroprotectant, antihypertension, antidiabetics, anticancer, geroprotective [1]. In addition they are calcium channels blockers and also act as therapeutic agents [2–6]. It is also used as laser dyes having very high efficiencies of photo initiators [7, 8]. In view of the significant biological activity associated with the acridine derivatives, various methods have been reported for their synthesis. Most common among these involve the one-pot three component condensation of cyclic 1,3-dicarbonyls, arylaldehydes and ammonium acetate or anilines. For example, Shen et al. have reported one-pot three-component synthesis of 1,8-dioxo-9,10-diaryl-decahydroacridines in water in the presence of the Brønsted acidic imidazolium salts containing perfluoroalkyl tails [9], Aday et al. have reported the synthesis of acridinedione derivatives via a one-pot multi-component condensation of dimedone, various aromatic aldehydes, and various aromatic amines using highly monodisperse platinum nanoparticles supported onto reduced graphene oxide (Pt NPs@rGO) as a recyclable heterogeneous catalyst [10] and Vaid et al. have prepared MPTMS-functionalized silica immobilized with biphenyl-2,2'-dioic acid as an efficient catalyst for the one-pot synthesis of acridine-1,8-dione derivatives [11]. Here, we wish to report the synthesis, characterization and crystal structure of a fully functionalized acridine derivative, namely 3,3,6,6-tetramethyl-9-(4-methoxyphenyl)-10-(4-chlorophenyl)-1,8-dioxodecahydroacridine dimethyl sulfoxide (Fig. 1) using a green procedure which involve the one-pot reaction of 4-methoxybenzaldehyde, dimedone and 4-chloroaniline in presence of $C_{Star}@SiO_2$-TfOH [12]. This method have several advantages such as low catalyst loading, use of non-toxic, highly active, stable and green solid acid catalyst, cleaner reaction profile, simple work-up procedure, good to excellent yield, recyclability and use of environmentally benign solvent.

EXPERIMENTAL

Synthesis

In a typical experimental procedure, a mixture of 4-methoxybenzaldehyde (1 mmol), dimedone (2 mmol), 4-chloroaniline (1 mmol) and $C_{Star}@SiO_2$-TfOH (0.1 g) were dispersed in water (5 mL) and stirred at 80°C for an appropriate time. After completion of the reaction as monitored by TLC, the catalyst was separated by filtration and washed with ethyl acetate (3 × 10 mL) and deionized water (3 × 10 mL). It was dried in an oven at 80°C for 24 h. The reaction mixture was cooled to room temperature, diluted with ethyl acetate (20 mL)

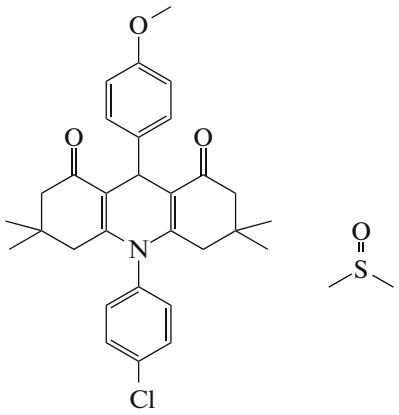

Fig. 1. Chemical structure of 3,3,6,6-tetramethyl-9-(4-methoxyphenyl)-10-(4-chlorophenyl)-1,8-dioxodecahydroacridine dimethyl sulfoxide (**I**).

and washed with brine solution followed by drying over anhydrous Na_2SO_4. Finally, the product was obtained after removal of the solvent under reduced pressure followed by crystallization in ethyl acetate (yield 92%; m.pt. 254–255°C).

Single crystals suitable for X-ray diffraction were obtained by slow evaporation of DMSO solution.

Characterization

Yellow coloured crystals; m.pt. 254–255°C; (lit. m.pt. 255–257°C); [10] ^{1}H NMR (400 MHz, DMSO-*d6*): δ 0.72 (s, 6H, $2CH_3$), 0.89 (s, 6H, $2CH_3$), 1.74–1.78 (d, 2H, J = 16 Hz, CH_2), 1.98–2.02 (d, 2H, J = 16 Hz, CH_2), 2.16–2.21 (m, 4H, $2CH_2$), 3.69 (s, 3H, OCH_3), 4.96 (s, 1H, CH), 6.79–6.81 (d, 3H, J = 8 Hz, ArH), 7.19–7.21 (d, 3H, J = 8 Hz, ArH), 7.67–7.69 (d, 2H, J = 8 Hz, ArH); ^{13}C NMR (100 MHz, DMSO-*d6*): δ 26.4, 29.8, 32.1, 32.4, 41.4, 50.1, 113.1, 117.4, 128.5, 130.1, 130.8, 139.1, 145.8, 151.1, 156.8, 195.9; MS (ESI): 488.24 [M – 1], 491.24 $[M + 2]^+$.

Crystal Structure Determination and Refinement

The crystallographic data are summarized in Table 1. The molecular structure solution was obtained by direct method procedure as using SHELXT [13]. The cell dimensions were determined by least-squares fit of angular settings of 2544 reflections in the θ range 2.1170° to 27.3560°. The value of R_{int} = 0.0215 and R_σ = 0.0473 shows satisfactory quality of the data. Five cycles of full-matrix least-squares refinement was carried out and it brought the final R-factor to 0.0587. All non-hydrogen atoms of the molecule were located in the best E-map and refined in anisotropic approximation using SHELXS [13]. The position of all the Hydrogen atoms bonded to C atoms were geometrically fixed and allowed to ride on the corresponding non-H atoms (C–H = 0.93–0.96 Å, and U_{iso}(H) = 1.5U_{eq} of the attached C atoms for methyl groups and 1.2U_{eq}(C) for other H atoms. The residual electron density in the final difference Fourier map between $-0.491 < \Delta\rho < 0.773$. The geometry of the title molecule was calculated using WinGX [14], PARST [15], and PLATON [16] software. Hirshfeld surfaces are mapped using d_{norm}, the shape index and curvature presented in this paper were generated using Crystal Explorer 17 [17].

Crystallographic information has been deposited with Cambridge Crystallographic Data Centre, CCDC no. 2009450. The data can be obtained from through www.ccdc.cam.ac.uk/data_request/cif by

Table 1. Crystallographic characteristics, details of X-ray data collection and structure refinement parameters for compound (**I**)

Chemical formula	$C_{30}H_{32}O_3ClNS{\cdot}C_2H_6OS$
System, sp. gr., Z	Triclinic, $P\bar{1}$, 2
a, b, c Å	9.9023(9), 11.5157(9), 13.8886(11)
α, β, γ deg	73.878(7), 75.465(7), 83.857(7)
V, Å^3	1471.6(2)
D_x, g cm^{-3}	1.282
Radiation, λ, Å	MoK_α, 0.71073
μ, mm^{-1}	0.238
T, K	293(2)
Sample size, mm	0.30 × 0.20 × 0.20
Diffractometer	Rigaku Oxford CCD plate diffractometer
Scan mode	ω scan
Absorption correction	Multi-scan
T_{min}, T_{max}	0.97298, 1.00000
θ_{min}, θ_{max}, deg	1.842°, 26.000°
h, k, l ranges	$-12 \le h \le 11$, $-11 \le k \le 14$, $-17 \le l \le 16$
Number of reflections:	
measured/unique ($N1$)	7610/5720
R_{int}/with $I > 2\sigma(I)$ ($N2$)	0.0215/4137
Refinement method	Full matrix least squares on F^2
Number of refined parameters	359
$R1$/$wR2$ relative to $N1$	0.0821/0.1518
$R1$/$wR2$ relative to $N2$	0.0587/0.1321
S	1.021
$\Delta\rho_{max}/\Delta\rho_{min}$, e/Å^3	0.773/–0.491
Programs	SHELXT [13], SHELXL [13], PARST [15], PLATON [16], ORTEP [18]

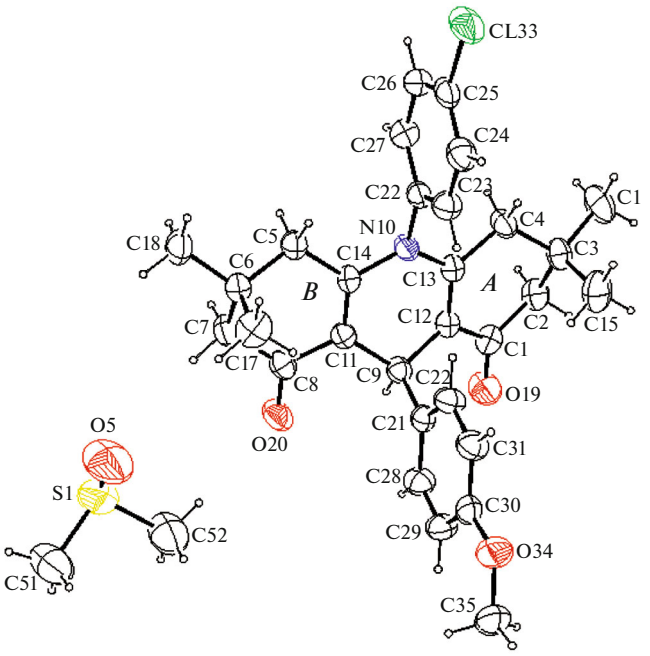

Fig. 2. The structure of the crystal (**I**), displacement ellipsoids are drawn at 50% probability level.

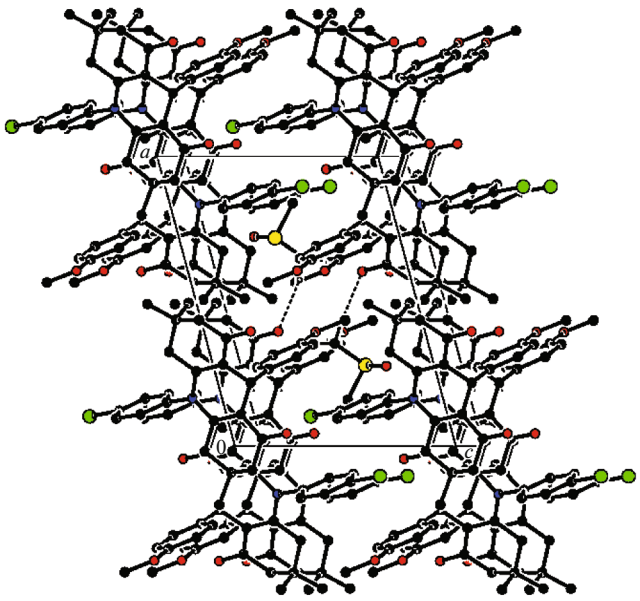

Fig. 3. Packing view of molecules down to *b*-axis (noninteracting hydrogen atoms are omitted for clarity).

e-mailing data request@ccdc.cam.ac.uk, or by contacting The Cambridge Crystallography Data Centre, 12 Union Road, Cambridge, CB2 IEZ, UK. Fax: +44(0) 1223-336033.

RESULTS AND DISCUSSION

The molecular structure containing atomic labeling of the asymmetric unit, $C_{30}H_{32}O_3ClNS{\cdot}C_2H_6OS$ is shown in Fig. 2 (ORTEP) [18] and the packing diagram as generated using PLATON [16] is shown in Fig. 3. X-ray structure analysis has shown that the asymmetric unit is one molecule of the compound and one molecule of solvent DMSO. Most of the geometrical parameter are normal [19] and are in close agreement with the reported solvent-free polymorph structure ($C_{30}H_{32}ClNO_3$) [20]. An overlay diagram for ($C_{30}H_{32}ClNO_3$) (**II**) and for molecule (**I**) is shown in Fig. 4. Significant bond lengths and bond angles are listed in Table 2.

The molecule (**I**) consists of two cyclohexene rings *A* and *B* bridged with pyridine unit through double bond lengths of C12–C13 = 1.354(3) Å and C11–C14 = 1.356(3) Å. In these cyclohexene rings *A* and *B*, the bond length of C1–O19 = 1.233(3) Å and C8–O20 = 1.227(3) Å are of typical C=O bond lengths. The geometrical parameters of nitrogen atom in the pyridine unit are N10–C13 = 1.400(3) Å, N10–C14 = 1.402(3) Å, N10–C22 = 1.449(3) Å; C13–N10–C14 = 120.0(2)° which on comparison with the reported polymorph shows quiet closeness (1.405(4) Å, 1.398(4) Å, 120.1(3)°, respectively). Moreover, the exocyclic bond angles at the ring junctions N10–C13–C4 = 116.7(2)°, N10–C14–C5 = 117.1(2)°, C9–C11–C8 = 118.4(2)°, and C9–C12–C1 = 118.6(2)° are significantly lesser than ideal value of 120°. All the endocyclic bond angles of the anisole and chlorobenzene rings lies between 113.7(2)° to 123.3(2)° and 108.0(2)° to 123.1(2)°, respectively. Whereas in case of pyridine ring all the bond angles lies in the range of 119.7(2)° to 121.6(2)°. The oxymethane group attached C30 atom of anisole ring have O34–C30 = 1.370(3) Å and O34–C35 = 1.432(4) Å which are quite similar to bond lengths of 1.387(4), 1.420(4) Å in reported structure ($C_{30}H_{32}ClNO_3$) (**II**) [19]. In the chlorobenzene ring C25–Cl33 bond length is 1.741(3) Å. In the title mol-

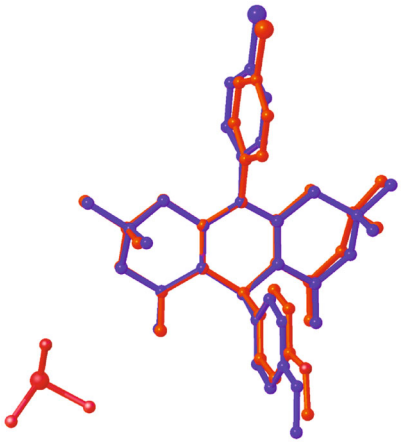

Fig. 4. Overlay diagram for ($C_{30}H_{32}ClNO_3$) (**II**) and molecule of (**I**).

Table 2. Selected bond lengths and angles for compound (**I**)

Bond	*d*, Å	Bond	*d*, Å
C1–C2	1.504(4)	C6–C18	1.536(4)
C2–C3	1.522(4)	C6–C7	1.529(4)
C3–C15	1.523(4)	C7–C8	1.504(4)
C3–C16	1.536(4)	C8–C11	1.459(3)
C3–C4	1.533(4)	C11–C9	1.507(3)
C4–C13	1.502(3)	C9–C12	1.512(3)
C13–C12	1.354(3)	C9–C21	1.526(4)
C13–N10	1.400(3)	C12–C1	1.459(3)
N10–C22	1.449(3)	O19–C1	1.233(3)
N10–C14	1.402(3)	O20–C8	1.227(3)
C14–C5	1.505(3)	C30–O34	1.370(3)
C14–C11	1.356(3)	O34–C35	1.432(4)
C5–C6	1.529(4)	C25–CL33	1.741(3)
C6–C17	1.528(4)		
Angle	ω, deg	Angle	ω, deg
C1–C2–C3	113.7(2)	C5–C6–C17	110.2(2)
C2–C3–C4	108.1(2)	C5–C6–C18	109.4(2)
C2–C3–C15	110.4(3)	C17–C6–C18	109.2(2)
C2–C3–C16	109.6(2)	C5–C6–C7	108.0(2)
C15–C3–C16	109.2(2)	C7–C6–C17	110.2(2)
C15–C3–C4	110.6(2)	C7–C6–C18	109.9(2)
C16–C3–C4	108.9(2)	C6–C7–C8	113.7(2)
C3–C4–C13	113.6(2)	C7–C8–C11	118.4(2)
C4–C13–C12	123.3(2)	O20–C8–C7	120.8(2)
C4–C13–N10	116.7(2)	O20–C8–C11	120.8(2)
C12–C13–N10	120.0(2)	C14–C11–C9	121.9(2)
C13–C12–C1	119.8(2)	C8–C11–C9	118.4(2)
C13–C12–C9	121.6(2)	C14–C11–C8	119.8(2)
C13–N10–C14	120.0(2)	C11–C9–C12	108.7(2)
C11–C14–N10	119.7(2)	C9–C12–C1	118.6(2)
N10–C14–C5	117.1(2)	C12–C1–C2	118.2(2)
C11–C14–C5	123.1(2)	C5–C6–C17	110.2(2)
C14–C5–C6	114.0(2)		

ecule, the orientation of anisole and chlorobenzene rings with respect to the attached pyrazole and pyran rings is characterized by torsion angles C13–N10–C22–C27 = 92.3(3)° and C11–C9–C21–C32 = –65.6(3)° both in (+sc) configuration.

Here the central pyridine ring and both the cyclohexene rings *A* and *B* are non-planar having total puckering amplitudes, Q_T, of 0.2932(2), 0.4660(1), 0.4607(2) Å, respectively. The central pyridine ring shows flattened boat conformation, where atom C9 shows maximum deviation of –0.5509(3) from plane of mean deviation. Both the cyclohexene rings *A* and *C* shows envelope conformation with maximum deviation for C7 and C2 of 0.5429(3) and 0.5468(3) from planarity. The puckering parameters are $\phi = 179.31(2)°$ and $\theta = 73.57(2)°$ for pyridine ring, $\phi = 469.60(9)°$ and $\theta = 56.52(3)°$ for cyclohexene ring *A*, and $\phi = 250.37(6)°$ and $\theta = 123.48(2)°$ for cyclohexene ring *B* [21]. Both anisole ring and chlorobenzene ring are in perpendicular configuration with respect to the acridine ring system, as can be seen from the dihedral angle of 89.70(6)° and 89.02(6)°, respectively.

The DMSO solvent molecule plays an important role in the stability of the crystal structure. The crystal structure is stabilized by hydrogen bonds involving the solvent molecule, where carbon atom C52 of DMSO solvent acts as donor via H52*A* and H52*B* to oxygen atom O20 of the anisole ring, in C52–H52*A*···O32 and C52–H52*B*···O31 interaction. In addition the molecular packing is also stabilized with the help of weak C–H···π and Vander Waal's forces. Fig. 3 shows the molecular packing in the unit cell viewed down the *b*-axis (PLATON program) [16]. The geometry of these interactions is presented in Table 3.

HIRSHFELD SURFACE ANALYSIS

In order to carry out the Hirshfeld surface analysis CrystalExplorer 17 program was used, for which Crystallographic information file (CIF) was used as input. The molecular Hirshfeld surfaces are created by splitting space in the crystal into a number of regions based on electronic distribution of atoms along the crystal. Figure 5 shows a comparison of Hirshfeld 3D surfaces of d_{norm}, shape index, curvedness in addition to 2D fingerprint plots for crystal (**I**) and (**II**), which are achieved by mapping d_{norm} over the Hirshfeld surface in the range –0.2377 to 1.5625. It indicates intermolecular interactions with the solvent DMSO molecule for (**I**). Transparent surfaces are shown to visualize functional groups present within the surface. Color areas symbolize closer contacts with a negative d_{norm} value, exactly the comparable distance when separating a van der Waals contact and zero or more distant contacts with a positive d_{norm} value, respectively. Large circular spots on d_{norm} surfaces indicate hydrogen bonds and other spots indicate bonding between other atoms. These regions correspond to positive and negative electrostatic potentials, respectively, which reveal the contribution of donor and acceptor interactions. The shape index on the Hirshfeld surface can be used to recognize complementary bumps and hollows, where the bump-shape corresponds to donor, and the hollow represents the acceptor of intermolecular interactions, and these stains here represents the regional molecular surfaces having contact and C–H···π interactions present in the crystal structure [22, 23].

2D fingerprint graphs are plotted by accumulating (d_i, d_e) pairs. The coloring for each collection has been taken as a function of the fraction over surface points,

Table 3. Geometry of intermolecular and intramolecular interactions for compound **(I)**

D–H···*A*	*D*–H, Å	H···*A*, Å	*D*···*A*, Å	θ(*D*–H···*A*), deg
C52–H52*A*···O20^{i}	0.96	2.57	3.524(4)	173
C52–H52*B*···O20^{ii}	0.96	2.41	3.332(5)	162
C35–H35*A*···Cg4^{iii}	0.96	2.70	3.512(4)	142

Symmetry codes: (*i*) $1-x, 1-y, 1-z$, (*ii*) x, y, z, (*iii*) $1-x, -y, 1-z$, where Cg4 is (C21/C28/C29/C30/C31/C32).

varying from several points to average and numerous points. A sketch of the full fingerprint is shown in light color [24]. The comparison of percentage contribution to the total Hirshfeld surface area, are shown in Table 4, where the H···H interaction is followed by O···H/H···O interaction as leading intermolecular interactions, in both crystals **(I)** and **(II)**.

CONCLUSIONS

In summary, 3,3,6,6-tetramethyl-9-(4-methoxyphenyl)-10-(4-chlorophenyl)-1,8-dioxodecahydroacridine was synthesized via one-pot three component reaction in water at 80°C using C_{Star}@SiO_2-TfOH as a highly active, stable and green solid acid catalyst. The synthesized compound was characterized by using various spectroscopic techniques such as ^{1}H-NMR, ^{13}C-NMR and mass spectral analysis. Suitable single crystals were obtained by slow evaporation in DMSO solution, whose strucutre was elucidated using X-ray

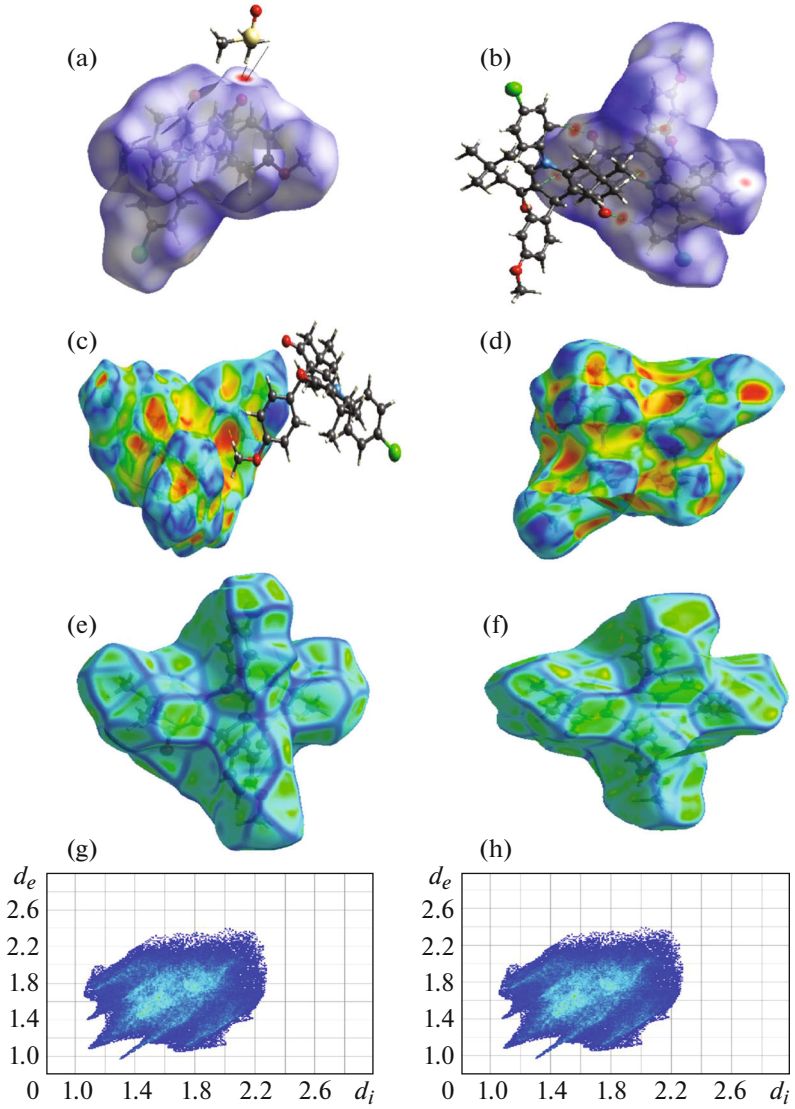

Fig. 5. A comparision of Hirshfeld surfaces mapped with d_{norm} for **(I)** (a), d_{norm} for **(II)** (b), shape index for **(I)** (c), shape index for **(II)** (d), curvedness for **(I)** (e), curvedness for **(II)** (f) and 2D finger print plots for **(I)** (g), 2D finger print plots for **(II)** (h).

Table 4. Summary of the various intermolecular contacts contributed to the Hirshfeld surface

Intermolecular interaction	Contribution, % (**II**)	Contribution, % (**I**)
Cl···O/O···Cl	0.1	0.3
Cl···C/C···Cl	1.6	3.0
Cl···H/H···Cl	9.9	7.0
S···H/H···S	—	1.2
N···H/H···N	0.1	0.3
O···C/C···O	0.3	0.2
O···H/H···O	16.0	16.9
C···C	1.5	1.8
C···H/H···C	10.9	10.9
H···H	59.5	58.2

diffraction. The compound (**I**) crystallizes in the triclinic system with space group $P\bar{1}$. The pyridine and cyclohexene rings adopt boat and envelope conformation respectively. Solvent molecules played an incomparable role in the formation of supramolecular structure through hydrogen bonded network which was understood in detail through Hirshfeld surface analysis.

ACKNOWLEDGMENTS

One of the authors (VKG) is thankful to University of Jammu, Jammu, India for financial support under RUSA 2.0.

REFERENCES

1. A. Rajacka, K. Yuvaraju, C. Praveen, et al., J. Mol. Catal. A **370**, 197, (2013).
2. B. Wysocka-Skrzela and A. Ledochowski, Rocz. Chem. **50**, 127 (1976).
3. A. Nasim and T. Brychey, Mutat. Res. **65**, 261 (1979).
4. U. Thull and B. Testa, Biochem. Pharmacol. **47**, 2307 (1994).
5. E. Reil, M. Scoll, K. Masson, et al., Biochem. Soc. Trans. **22**, 62s (1994).
6. Y. Mandi, K. Regely, I. Ocsovszky, et al., Anticancer Res. **14**, 2633 (1994).
7. S. Kumar and K. N. Singh, J. Heterocycl. Chem. **48**, 69 (2011).
8. X. Fan, Y. Li, X. Zhang, G. Qu, et al., Heteroatom Chem. **18**, 786 (2007).
9. W. Shen, L. M. Wang, H. Tian, et al., J. Fluor. Chem. **130**, 522 (2009).
10. B. Aday, Y. Yildiz, R. Ulus, et al., New J. Chem. **40**, 748 (2016).
11. R. Vaid, M. Gupta, and V. K. Gupta, J. Iran. Chem. Soc. **14**, 2199 (2017).
12. S. Sharma, H. Sharma, S. Sharma, S. Paul, et al., ChemistrySelect **5**, 2201 (2020).
13. G. M. Sheldrick, Acta Crystallogr. A **71,** 3 (2015).
14. L. J. Farrugia, J. Appl. Crystallogr. **45**, 849 (2012).
15. M. Nardelli, J. Appl. Crystallogr. **28,** 659 (1995).
16. A. L. Spek, Acta Crystallogr. D **65,** 148 (2009).
17. M. J. Turner, J. J. McKinnon, S. K. Wolff, et al., *CrystalExplorer17* (Univ. of Western Australia, 2017).
18. L. J. Farrugia, J. Appl. Crystallogr. **30**, 565 (1997).
19. F. H. Allen, O. Kennard, D. G. Watson, et al., J. Chem. Soc., Perkin Trans. **2,** S1 (1987).
20. Y. Chen, W.-J. Hao, Z.-Q. Tang, B. Jiang, and C.-M. Li, Acta Crystallogr. E **63**, o3934 (2007).
21. D. Cremer and A. J. Pople, J. Am. Chem. Soc. **97**, 1354 (1975).
22. M. A. Spackman and D. Jayatilaka, CrystEngCommun **11**, 19 (2009).
23. R. Hoffmann Inc. (New York, 1988).
24. J. J. McKinnon, A. S. Mitchell, and M. A. Spackman, Chemistry A **4**, 2136 (1998).